THE JOURNAL OF PHYSICAL CHEMISTRY C

Article

pubs.acs.org/JPCC

Mechanistic Characteristics of Metal-Assisted Chemical Etching in GaAs

Ho-Yuen Cheung,[†] Hao Lin,[‡] Fei Xiu,[‡,∥] Fengyun Wang,[§] SenPo Yip,[‡,∥] Johnny C. Ho,*[,‡,∥] and Chun-Yuen Wong*[,†]

[†]Department of Biology and Chemistry, City University of Hong Kong, 83 Tat Chee Avenue, Kowloon, Hong Kong

[‡]Department of Physics and Materials Science, City University of Hong Kong, 83 Tat Chee Avenue, Kowloon, Hong Kong

[§]Cultivation Base for State Key Laboratory, Qingdao University, No. 308 Ningxia Road, Qingdao, People's Republic of China

[∥]Shenzhen Research Institute, City University of Hong Kong, Shenzhen, People's Republic of China

Supporting Information

ABSTRACT: Because of the unique physical properties, various GaAs micro- and nanostructures have attracted increasing research attention for many technical applications such as solar cells, light-emitting diodes, and field-effect transistors. In this regard, numerous fabrication techniques have been explored, and among all, metal-assisted chemical etching is successfully applied to GaAs in order to achieve cost-effective, large-scale, and complex structures. However, the detailed explanations as well as the corresponding etching mechanism have not been reported until now or simply relied on the hole injection model of Si in order to explain the phenomenon. In this work, we perform a more systematic study to further explore and assess the etching phenomenon of GaAs employing the Au catalyst and the [$KMnO_4/H_2SO_4$] etch system. It is revealed that the anisotropic etching behavior of GaAs is predominantly due to the Au-induced surface defects at the Au/GaAs interface, which makes the particular area more prone to oxidation and thus results in the simple directional wet etching; for that reason, more anisotropic etch is obtained for the Au pattern with higher edge-to-surface-area ratio. All these findings not only offer additional insight into the MacEtch process of GaAs but also provide essential information on different etching parameters in manipulating this anisotropic wet etching to achieve the fabrication of complex GaAs structures for technological applications.

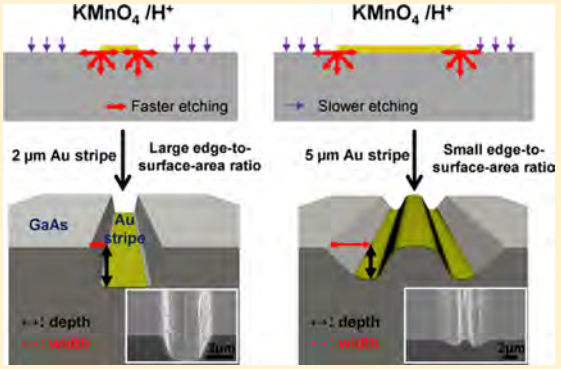

INTRODUCTION

In the past decades, because of the unique physical properties, III−V compound semiconductors have attracted extensive research and development interests for many technical applications such as solar cells, light-emitting diodes and field-effect transistors.[1−6] In particular, several types of GaAs micro- and nanostructures, with the high carrier mobility, appropriate direct bandgap, and superior solar spectrum absorption, have become promising candidates as active materials over their silicon counterparts for high-performance photovoltaics.[7−11] In this regard, different fabrication techniques, classified into "top-down" or "bottom-up" approaches, have been employed to achieve various GaAs structures, including nanowires, microwires, and micropillars, etc.[12−17] Generally, bottom-up methods rely on the additive growth processes to obtain the finished structures, in which it could be difficult to govern their crystalline quality, orientation, and dimension precisely.[18,19] While top-down techniques adapt the removal processes in the starting substrate, it would make such geometrical and structural control easier in the completed structures.[20,21] For example, reactive ion etching (RIE) has been commonly utilized to attain high-aspect ratio structures with well-controlled morphologies; however, the substantial processing cost, low throughput, chemical contamination, and the induced surface roughness may potentially restrict the practical implementation of these structures.[20,22] At the same time, another top-down method, known as metal-assisted chemical etching (MacEtch) with the first demonstration in silicon, exploits noble metals (e.g., Ag, Au, and Pt) as the catalysts predeposited onto the starting substrates, which can introduce anisotropic wet etching to achieve the same high-aspect ratio structures in the large scale but in a much mild chemical and processing condition as compared with RIE.[23,24]

Since then, in addition to silicon, MacEtch has also been applied to other material systems, including GaAs.[12,17,25−32] Although several GaAs structures were successfully illustrated employing the Au catalysts and etch system [$KMnO_4/H_2SO_4$], the detail explanations as well as the etching mechanism have not been reported until now or simply relied on the hole injection model of Si in order to explain the phenomenon.[17] As

Received: January 27, 2014
Revised: March 14, 2014
Published: March 15, 2014

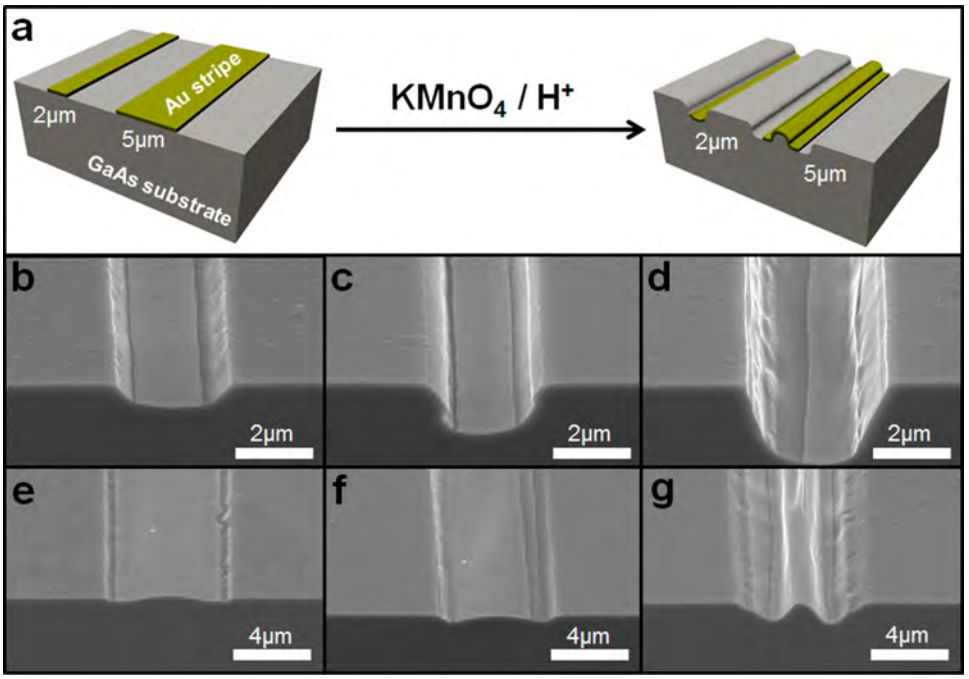

Figure 1. Effect of different Au stripe widths and etching durations on the etching morphology of GaAs substrates. (a) depicts the schematic illustration of the etching process. (b), (c), and (d) show the SEM images of U-shaped pits formed by 2 μm width Au stripe induced etching for 1, 3, and 5 min, respectively. (d), (e), and (f) illustrate the SEM images of W-shaped pits formed by 5 μm width Au stripe induced etching for 1, 3, and 5 min, respectively. Etching conditions: $KMnO_4$ concentration = 15 mM; process temperature = 45 °C.

Ulrich Gösele and co-workers have questioned previously, the etching characteristics of Ga and As are entirely different from the one of Si such as the drastic difference in their chemical potential at the atomic level; it may not be applicable to elucidate this etching behavior based on the Si model.[33] As a result, it is necessary to investigate and understand all these etching details, which is essential in controlling and manipulating this MacEtch process for more complicated GaAs structures for the practical utilization. Here, we perform a more systematic study to further explore and assess the etching phenomenon of GaAs with the presence of Au catalyst under the [$KMnO_4/H_2SO_4$] etch system. Based on the experimental observation, it is revealed that the anisotropic etching behavior of GaAs is predominantly due to the Au-induced surface defects at the Au/GaAs interface, which makes the particular area more prone to oxidation and thus results in the simple directional wet etching; for that reason, more anisotropic etch is obtained for the Au pattern with higher edge-to-surface-area ratio. These findings not only offer additional insight into the MacEtch process of GaAs but also provide essential information on different etching parameters in manipulating this anisotropic wet etching to achieve the fabrication of cost-effective, large-scale, and complex GaAs structures for technological applications.

EXPERIMENTAL SECTION

All the chemical reactions were performed under an ambient atmosphere unless otherwise stated. Potassium permanganate ($KMnO_4$) was purified by recrystallization in dark,[34] and solvents were used as received. Epi-ready Si-doped (100) GaAs wafers, with a doping concentration of (2.5−4) × 10^{18} cm^{-3} commonly utilized in the MacEtch studies of GaAs,[12,17,25−28] were purchased from HSA Material Company Limited. The wafers were thorough cleaned with the sonication in deionized water (DI), acetone, and anhydrous ethanol sequentially for 5 min each, followed by blow-drying under a stream of nitrogen. Then microscale Au stripe patterns, with the stripe length of 100 μm and variable widths of 2, 5, and 56 μm, were prepared on the GaAs surface as catalysts using the conventional photolithography and lift-off processes. Specifically, 20 nm thick Au thin films were deposited by the electron-beam evaporation. Next, the etchant was prepared by dissolving $KMnO_4$ in a H_2SO_4 (98%)/H_2O mixture (1:9 v/v). The GaAs substrates with the Au stripe patterns were etched by the acidified $KMnO_4$ solution for 5 min without stirring while at that point washed with DI and blow-drying with nitrogen. All the samples were subsequently characterized by scanning electron microscopy (SEM, FEI Company, Hillsboro, OR/Philips XL30, Philips Electronics, Amsterdam, The Netherlands).

RESULTS AND DISCUSSION

In this work, the etching parameters were mainly varied by adapting different etchant concentrations (5, 10, and 15 mM $KMnO_4$), process temperatures (25, 35, 45, and 55 °C), and etching durations (1−5 min in the increment of 1 min step). Considering the instability of $KMnO_4$ in the presence of visible light, $KMnO_4$ was purified by recrystallization in the dark before use.[34] Figure 1 shows the schematic illustration of this etching process as well as the effect of different Au stripe widths and etching times on the etching morphologies of GaAs substrates, holding the etchant concentration and temperature constant. It is obvious that when the 2 μm wide Au stripe patterned samples were etched for the longer duration, the Au-covered region were eaten down more faster into the GaAs substrates, resulting in both vertical and lateral etching, and giving the U-shaped pits, which indicates the catalytic etching induced by the Au strips (Figure 1b−d). Notably, when the

dx.doi.org/10.1021/jp500968p | J. Phys. Chem. C 2014, 118, 6903−6908

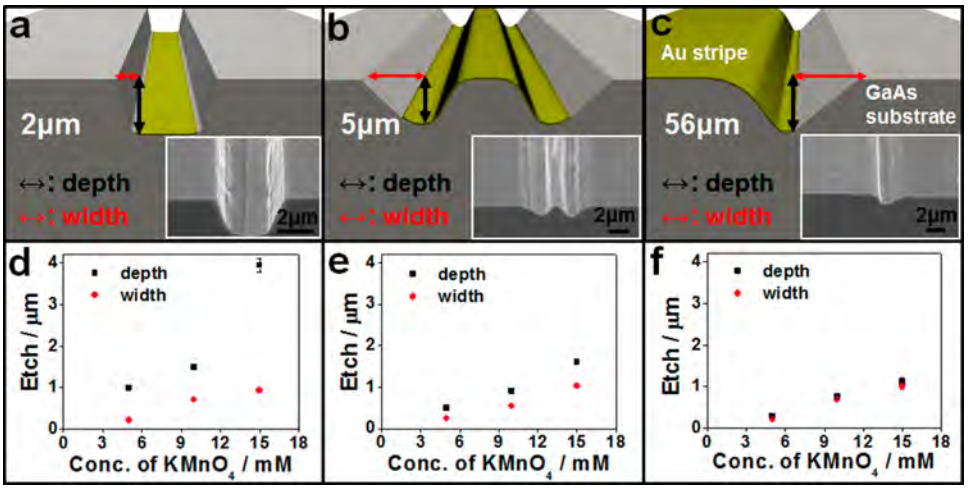

Figure 2. Effect of different concentration of etchant on the vertical-etch depths and lateral etch widths. (a), (b), and (c) illustrate the graphical representation of vertical-etch and lateral-etch in MacEtch process while (d), (e), and (f) demonstrate the etched depths and widths as a function of the etchant concentration among the samples with Au stripe widths of 2, 5, and 56 μm, respectively. Etching conditions: time = 5 min; temperature = 45 °C. Each data point is averaged over six samples, and the error bars are constructed by the standard error of mean.

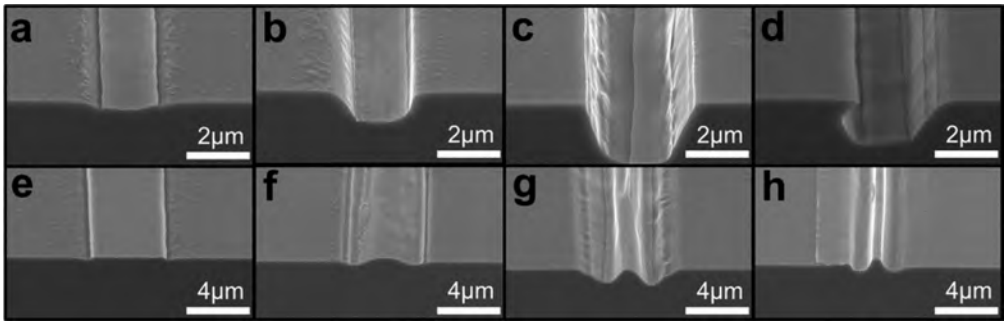

Figure 3. Effect of different process temperatures on the MacEtch process of GaAs. (a), (b), (c), and (d) show the SEM images of etching performed with the samples of 2 μm width Au stripes while (e), (f), (g), and (h) give the SEM images of etching performed with the samples of 5 μm Au stripes at the temperature of 25, 35, 45, and 55 °C, respectively. Etching conditions: time = 5 min; $KMnO_4$ concentration = 15 mM.

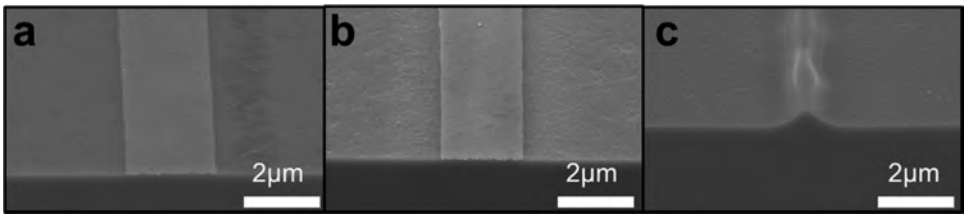

Figure 4. Control experiments for the 2 μm stripe width for the 5 min etching at 45 °C: (a) 1:9 H_2SO_4:H_2O, (b) $KMnO_4$ in neutral medium, and (c) Au pattern replaced by the SiO_2 pattern.

etching was performed more than 5 min, the Au strip started to delaminate from the substrate surface due to the inadequate adhesion; as a result, no further etching could be performed. On the other hand, when stripe width was increased to 5 μm, the etching is surprisingly more pronounced in the edge region, forming the W-shaped pits (Figure 1e–g).

In order to characterize this etching morphology more quantitatively, two parameters, namely, the vertical-etch depth (black arrows) and lateral-etch width (red arrows), are defined and assessed during the processing (Figure 2a–c). At the same time, Figure 2d–f summarizes the effect of different etchant concentration on various Au stripe widths in this MacEtch process (see the experimental details in Supporting Information Figure S1). It is found that the vertical-etch depths are always larger than the lateral-etch widths among all etchant concentrations in the case with Au stripe width of 2 μm, but these two values become very similar in the cases with stripe widths of 5 and 56 μm. Notably, the etching rates, especially the vertical ones, are observed significantly larger in the samples with the 2 μm stripe width and higher etchant concentration as compared with the wider stripes, suggesting that the faster vertical etch (i.e., more anisotropy) is resulted in the Au patterns with higher edge-to-surface-area ratio. Moreover, the effects of temperature for this etching manner are also being considered and evaluated in Figure 3. Little or insignificant etching could be observed for all dimensions of the Au stripe at room temperature (25 °C). The etching effect starts to become apparent when the temperature is increased to 35 °C or beyond. It is expected that faster etching would be occurred at higher temperatures due to the enhanced reaction rate. Above

dx.doi.org/10.1021/jp500968p | J. Phys. Chem. C 2014, 118, 6903–6908

45 °C, although the Au stripe pattern began to delaminate from the substrate surface at this temperature, it is still clear that the W-shaped pits are formed in this etching, again confirming the more anisotropic etch induced by the Au stripes patterned with the higher edge-to-surface-area ratio.

To shed light verifying the role of the all substances (e.g., Au, $KMnO_4$, and H_2SO_4, etc.) in this etching process, several control experiments were performed: (a) substrate was placed in a 1:9 H_2SO_4/H_2O solution without the etchant, (b) substrate was placed in the etchant without H_2SO_4, and (c) the Au stripes were replaced by SiO_2 stripes. Experiments a and b are used to determine the effect of each chemical agent during the etching process while experiment c is hired to assess the effect of the etchant for the bare substrate without the Au catalyst. All these control results are compiled in Figure 4. Specifically, no observable change was observed for the samples processed in the solution without the etchant (Figure 4a). Also, neither U-shaped nor W-shaped pits were found on the samples treated without H_2SO_4 while the surface roughness for the nonpatterned region got increased only (Figure 4b). Furthermore, when the SiO_2 stripes were utilized in the etching, they served as the mask to allow uncovered region being etched (Figure 4c). Even when the etchant concentration was changed, the oxide stripe would still be performed as the protective mask (Supporting Information Figure S2).

On the basis of the above experimental findings, the MacEtch mechanism in this work can be proposed as a combination of the oxidation of GaAs by $KMnO_4/H^+$ to give Ga_2O_3[35] (eq 1) and the removal of Ga_2O_3 by acid (eq 2).

$$10GaAs_{(s)} + 16KMnO_{4(aq)} + 24H_2SO_{4(aq)} \rightarrow 5Ga_2O_{3(s)} + 10H_3AsO_{4(aq)} + 16MnSO_{4(aq)} + 8K_2SO_{4(aq)} + 9H_2O \quad (1)$$

$$Ga_2O_{3(s)} + 3H_2SO_{4(aq)} \rightarrow Ga_2(SO_4)_{3(aq)} + 3H_2O \quad (2)$$

Simultaneously, the anisotropic etching of the Au patterned substrates is likely originated from the different etching rate for different regions: the edge of the patterned region possesses faster etching rate than the nonpatterned area. A plausible explanation for this phenomenon would be due to the Au induces surface defects at the Au/GaAs interface, making the patterned area more prone to oxidation than the native GaAs. It is also consistent with the findings that the etching morphologies highly depend on the width of the Au stripes. The removal of substrates for the metal covered regions was due to the faster isotropic etching at the Au stripe edge as depicted in the schematic illustration of Figure 5. The resultant shapes were related to the ratio of the etching rate to the stripe width. The greater the ratio gives U-shaped pits and the smaller the ratio gives W-shaped pits. To summarize, the deposited Au film has two roles. For one thing, it acts as the protective mask to prevent substrate etching underneath the central part of metal patterns rather than being a catalyst; the role for Au film to protect the underlying substrate is more apparent at higher temperature (see Figure 3). For another, it induces surface defects leading to faster etching at the edge of the metal pattern. In other words, these defects lead to faster etching/oxidation of the GaAs in radial direction around the Au/GaAs interface (as illustrated by the red arrows in Figure 5), especially at a higher etchant concentration due to the faster reaction rate, and this initiates both vertical and lateral etching.

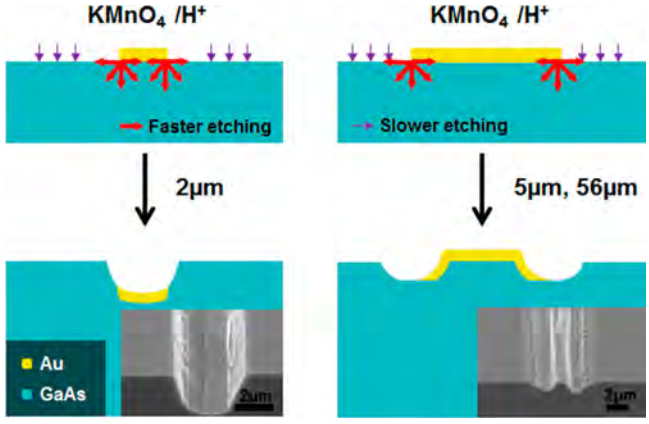

Figure 5. Proposed etching mechanism with different Au stripe widths. Faster etch rates are expected at the edge regions of Au stripes due to the Au-induced interface defects, yielding the higher anisotropic for the Au pattern with higher edge-to-surface-area ratio. Insets show the SEM images of the corresponding etching morphologies after the processing.

The faster etching rate in vertical direction than in lateral direction in the narrower stripe is probably due to the fact that the pit created is still in contact with the Au stripe throughout the etching process. All these elucidate the observation that more anisotropic etch is induced by the Au stripes pattern with the higher edge-to-surface-area ratio. More importantly, after the Au strip had been removed after etching, there was not any detectable Au residue (Supporting Information Figure S3), which indicates that Au contamination is minimal in this MacEtch process of GaAs.

CONCLUSIONS

In summary, we have performed a systematic investigation to explore and understand the mechanistic characteristics of metal-assisted chemical etching of GaAs employing the Au catalyst and the $[KMnO_4/H_2SO_4]$ etch system. It is revealed that the anisotropic etching behavior of GaAs is predominantly due to the Au-induced surface defects at the Au/GaAs interface, which makes the particular area more prone to oxidation and thus results in the simple directional wet etching; consequently, more anisotropic etch is obtained for the Au pattern with higher edge-to-surface-area ratio. These findings not only offer additional insight into the MacEtch phenomenon of GaAs but also provide essential information on different etching parameters in manipulating this anisotropic wet etching to achieve the fabrication of complex GaAs structures for technological applications.

ASSOCIATED CONTENT

Supporting Information

SEM images showing the effect of $KMnO_4$ concentration on the etching of samples with the 2 μm, 5 μm, and edge region of 56 μm Au stripe width; SEM images showing the effect of $KMnO_4$ concentration on the etching of samples with the 2 μm, 5 μm, and edge region of 56 μm SiO_2 stripe width. This material is available free of charge via the Internet at http://pubs.acs.org.

AUTHOR INFORMATION

Corresponding Authors

*E-mail johnnyho@cityu.edu.hk (J.C.H.).

*E-mail acywong@cityu.edu.hk (C.-Y.W.).

Notes

The authors declare no competing financial interest.

■ ACKNOWLEDGMENTS

This research was supported by the General Research Fund of the Research Grants Council of Hong Kong SAR, China, under Projects CityU 101210 and CityU 103911, the National Natural Science Foundation of China (grant 51202205), the Guangdong National Science Foundation (grant S2012010010725), and the Science Technology and Innovation Committee of Shenzhen Municipality (grant JCYJ20120618140624228) and was supported by a grant from the Shenzhen Research Institute, City University of Hong Kong.

■ REFERENCES

(1) Takei, K.; Kapadia, R.; Li, Y.; Plis, E.; Krishna, S.; Javey, A. Surface Charge Transfer Doping of III-V Nanostructures. *J. Phys. Chem. C* **2013**, *117*, 17845−17849.

(2) Nah, J.; Fang, H.; Wang, C.; Takei, K.; Lee, M. H.; Plis, E.; Krishna, S.; Javey, A. III−V Complementary Metal−Oxide−Semiconductor Electronics on Silicon Substrates. *Nano Lett.* **2012**, *12*, 3592−3595.

(3) Ho, J. C.; Ford, A. C.; Chueh, Y. L.; Leu, P.W.; Ergen, O.; Takei, K.; Smith, G.; Majhi, P.; Bennett, J.; Javey, A. Nanoscale Doping of InAs via Sulfur Monolayers. *Appl. Phys. Lett.* **2009**, *95*, 072108−1−3.

(4) Bosi, M.; Pelosi, C. The Potential of III-V Semiconductors as Terrestrial Photovoltaic Devices. *Prog. Photovoltaics* **2007**, *15*, 51−68.

(5) Bartel, T. P.; Specht, P.; Ho, J. C.; Kisielowskic, C. Phase Separation in $In_xGa_{1-x}N$. *Philos. Mag. A* **2007**, *87*, 1983−98.

(6) Ho, J. C.; Specht, P.; Yang, Q.; Xu, X.; Hao, D.; Weber, E. R. Effects of Stoichiometry on Electrical, Optical, and Structural Properties of Indium Nitride. *J. Appl. Phys.* **2005**, *98*, 93712−1−5.

(7) Krogstrup, P.; Jørgensen, H. I.; Heiss, M.; Demichel, O.; Holm, J. V.; Aagesen, M.; Nygard, J.; Morral, A. F. Single-Nanowire Solar Cells Beyond the Shockley−Queisser Limit. *Nat. Photonics* **2013**, *7*, 306−310.

(8) Mariani, G.; Scofield, A. C.; Hung, C.-H.; Huffaker, D. L. GaAs Nanopillar-Array Solar Cells Employing in-Situ Surface Passivation. *Nat. Commun.* **2013**, *4*, 1497.

(9) Liang, D.; Kang, Y.; Huo, Y.; Chen, Y.; Cui, Y.; Harris, J. S. High-Efficiency Nanostructured Window GaAs Solar Cells. *Nano Lett.* **2013**, *13*, 4850−4856.

(10) Han, N.; Wang, F. Y.; Yip, S. P.; Hou, J. J.; Xiu, F.; Shi, X. L.; Hui, A. T.; Hung, T. F.; Ho, J. C. GaAs Nanowire Schottky Barrier Photovoltaics Utilizing Au−Ga Alloy Catalytic Tips. *Appl. Phys. Lett.* **2012**, *101*, 013105.

(11) Mariani, G.; Wong, P.-S.; Katzenmeyer, A. M.; Léonard, F.; Shapiro, J.; Huffaker, D. L. Patterned Radial GaAs Nanopillar Solar Cells. *Nano Lett.* **2011**, *11*, 2490−2494.

(12) Mohseni, P. K.; Kim, S. H.; Zhao, X.; Balasundaram, K.; Kim, J. D.; Pan, L.; Rogers, J. A.; Coleman, J. J.; Li, X. GaAs Pillar Array-Based Light Emitting Diode Fabricated by Metal-Assisted Chemical Etching. *J. Appl. Phys.* **2013**, *114*, 064909.

(13) Dowdy, R. S.; Walko, D. A.; Li, X. Relationship Between Planar GaAs Nanowire Growth Direction and Substrate Orientation. *Nanotechnology* **2013**, *24*, 035304.

(14) Hou, J. J.; Wang, F. Y.; Han, N.; Xiu, F.; Yip, S. P.; Fang, M.; Lin, H.; Hung, T. F.; Ho, J. C. Stoichiometric Effect on Electrical, Optical and Structural Properties of Composition Tunable $In_xGa_{1-x}As$ Nanowires. *ACS Nano* **2012**, *6*, 9320−9325.

(15) Hou, J. J.; Han, N.; Wang, F. Y.; Xiu, F.; Yip, S. P.; Hui, A. T.; Hung, T. F.; Ho, J. C. Synthesis and Characterizations of Ternary InGaAs Nanowires by a Two-Step Growth Method for High-Performance Electronic Devices. *ACS Nano* **2012**, *6*, 3624−3630.

(16) Han, N.; Wang, F. Y.; Hui, A. T.; Hou, J. J.; Shan, G. C.; Fei, X.; Hung, T. F.; Ho, J. C. Facile Synthesis and Growth Mechanism of Ni-Catalyzed GaAs Nanowires on Non-Crystalline Substrates. *Nanotechnology* **2011**, *22*, 285607.

(17) Dejarld, M. T.; Shin, J. C.; Chern, W.; Chanda, D.; Balasundaram, K.; Rogers, J. A.; Li, X. Formation of High Aspect Ratio GaAs Nanostructures with Metal Assisted Chemical Etching. *Nano Lett.* **2011**, *11*, 5259−5263.

(18) Han, N.; Hou, J. J.; Wang, F. Y.; Yip, S. P.; Lin, H.; Fang, M.; Xiu, F.; Shi, X.; Hung, T. F.; Ho, J. C. Large-Scale and Uniform Preparation of Pure-Phase Wurtzite GaAs NWs on Non-Crystalline Substrates. *Nanoscale Res. Lett.* **2012**, *7*, 632.

(19) Joyce, H. J.; Wong-Leung, J.; Gao, Q.; Tan, H. H.; Jagadish, C. Phase Perfection in Zinc Blende and Wurtzite III−V Nanowires Using Basic Growth Parameters. *Nano Lett.* **2010**, *10*, 908−915.

(20) Morton, K. J.; Nieberg, G.; Bai, S.; Chou, S. Y. Wafer-Scale Patterning of Sub-40 nm Diameter and High Aspect Ratio (>50:1) Silicon Pillar Arrays by Nanoimprint and Etching. *Nanotechnology* **2008**, *19*, 345301.

(21) Hsu, C.-M.; Connor, S. T.; Tang, M. X.; Cui, Y. Wafer-Scale Silicon Nanopillars and Nanocones by Langmuir−Blodgett Assembly and Etching. *Appl. Phys. Lett.* **2008**, *93*, 133109−1−−3.

(22) Schmitt, S. W.; Schechtel, F.; Amkreutz, D.; Bashouti, M.; Srivastava, S. K.; Hoffmann, B.; Dieker, C.; Spiecker, E.; Rech, B.; Christiansen, S. H. Nanowire Arrays in Multicrystalline Silicon Thin Films on Glass: a Promising Material for Research and Applications in Nanotechnology. *Nano Lett.* **2012**, *12*, 4050−4054.

(23) Lin, H.; Cheung, H. Y.; Xiu, F.; Wang, F. Y.; Yip, S. P.; Han, N.; Hung, T. F.; Zhou, J.; Ho, J. C.; Wong, C. Y. Developing Controllable Anisotropic Wet Etching to Achieve Silicon Nanorods, Nanopencils and Nanocones for Efficient Photon Trapping. *J. Mater. Chem. A* **2013**, *1*, 9942−9946.

(24) Wang, F.; Yang, Q. D.; Xu, G.; Lei, N. Y.; Tsang, Y. K.; Wong, N. B.; Ho, J. C. Highly Active and Enhanced Photocatalytic Silicon Nanowire Arrays. *Nanoscale* **2011**, *3*, 3269−3276.

(25) Aizawa, M.; Cooper, A. M.; Malac, M.; Buriak, J. M. Silver Nano-Inukshuks on Germanium. *Nano Lett.* **2005**, *5*, 815−819.

(26) Li, X.; Kim, Y.-W.; Bohn, P. W.; Adesida, I. In-Plane Bandgap Control in Porous GaN through Electroless Wet Chemical Etching. *Appl. Phys. Lett.* **2002**, *80*, 980−1−3.

(27) Rittenhouse, T. L.; Bohn, P. W.; Adesida, I. Structural and Spectroscopic Characterization of Porous Silicon Carbide formed by Pt-Assisted Electroless Chemical Etching. *Solid State Commun.* **2003**, *126*, 245−250.

(28) Geng, X.; Duan, B. K.; Grismerb, D. A.; Zhao, L.; Bohn, P. W. Monodisperse GaN Nanowires Prepared by Metal-Assisted Chemical Etching with in-Situ Catalyst Deposition. *Electrochem. Commun.* **2012**, *19*, 39−42.

(29) Yasukawa, Y.; Asoh, H.; Ono, S. Site-Selective Chemical Etching of GaAs through a Combination of Self-Organized Spheres and Silver Particles as Etching Catalyst. *Electrochem. Commun.* **2008**, *10*, 757−760.

(30) Yasukawa, Y.; Asoh, H.; Ono, S. Site-Selective Metal Patterning/Metal-Assisted Chemical Etching on GaAs Substrate Through Colloidal Crystal Templating. *J. Electrochem. Soc.* **2009**, *156*, H777−H781.

(31) Yasukawa, Y.; Asoh, H.; Ono, S. Morphological Control of Periodic GaAs Hole Arrays by Simple Au-Mediated Wet Etching. *J. Electrochem. Soc.* **2012**, *159*, D328−D332.

(32) Yasukawa, Y.; Asoh, H.; Ono, S. Periodic GaAs Convex and Hole Arrays Produced by Metal-Assisted Chemical Etching. *Jpn. J. Appl. Phys.* **2010**, *49*, 116502-1−4.

(33) Huang, Z.; Geyer, N.; Werner, P.; de Boor, J.; Gösele, U. Metal-Assisted Chemical Etching of Silicon: A Review. *Adv. Mater.* **2011**, *23*, 285−308.

(34) Phillips, B. R.; Taylor, D. The Early Stages of the Thermal Decomposition of Potassium Permanganate−Potassium Perchlorate Solid Solutions. *J. Chem. Soc.* **1962**, 4242−4247.

(35) Shiota, I.; Motoya, K.; Ohmi, T.; Miyamoto, N.; Nishizawa, J. Auger Characterization of Chemically Etched GaAs Surfaces. *J. Electrochem. Soc.* **1977**, *124*, 155−157.